

1  
2  
3  
4  
5  
6  
7  
8  
9  
10  
11  
12  
13  
14  
15  
16  
17  
18  
19  
20  
21  
22  
23

---

# **An experimental approach to the optimization of the dosage of hydrogen peroxide for Fenton and photo-Fenton processes**

Xiangwei, Yu<sup>a</sup>, Somoza-Tornos, Ana<sup>a</sup>, Graells, Moisès<sup>a</sup>, Pérez-Moya, Montserrat<sup>a\*</sup>

<sup>a</sup>Department of Chemical Engineering. Universitat Politècnica de Catalunya. EEBE,  
Av. Eduard Maristany 16, 08019-Barcelona, \*corresponding author:

e-mail: [montserrat.perez-moya@upc.edu](mailto:montserrat.perez-moya@upc.edu) telf. +34 413 74 59

## **Abstract**

The determination of the hydrogen peroxide dosage scheme that minimizes hydrogen peroxide consumption while meeting the specified treatment outcome is crucial for Fenton and photo-Fenton processes. The challenge is building a methodology that provides the optimal dosage profile. However, the lack of detailed dynamic models prevents exploiting model-based optimization methods that have proved successful in other applications. Thus, this work addresses this challenge by providing a problem formulation identifying and discussing objectives and constraints, and the nature of the optimal solution. From this point, the work presents a novel dosage model and a consequent methodology aimed at experimentally optimizing the dosage profile along a discretized time horizon following recipe optimization concepts. The approach is parallel to the numerical solution of the model-based optimization problem posed by hydrogen peroxide dosage. The proposed methodology is validated in the remediation of a Paracetamol (PCT) solution, and the obtained results are assessed and discussed in regard of the evolution of the concentration of hydrogen peroxide, the contaminant (PCT), and Total Organic Carbon (TOC). The concentration of dissolved oxygen (DO), which is also monitored, allows providing a more comprehensive explanation of the nature of the process.

---

## 24 **Keywords**

25 Photo-Fenton; Hydrogen peroxide dosage; Recipe optimization; Experimental design; Dissolved oxygen  
26 monitoring; Hydrogen peroxide consumption

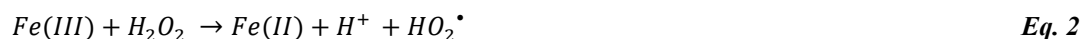
27

## 28 **1. Introduction**

29 The application of advanced oxidation processes (AOPs) to the degradation of recalcitrant organic matter  
30 has been extensively studied over the last decades. Among AOPs, the Fenton process, stemming from  
31 the work by Henry Fenton in the 1890s, has received increasing attention as it has proved to be highly  
32 efficient in the treatment of wastewaters containing non-biodegradable contaminants and producing  
33 extensive toxicity reduction. The advantages of the Fenton process are the need of a reagent easy to  
34 obtain, the flexibility of the operations, a short reaction time, and harmless by-products (Pignatello et al.,  
35 2006). In addition, the Fenton process takes place at ambient temperature and barometric pressure.

36 In the Fenton process, hydrogen peroxide ( $H_2O_2$ ) and a Fe(II) catalyst produce highly reactive hydroxyl  
37 radicals ( $HO^\bullet$ ), (Eq. 1-2), which unselectively react with organic matter, concomitantly with the  
38 oxidation of Fe (II) into Fe(III).

39 The presence of UV-vis light ( $\lambda \leq 580nm$ ) allows reducing Fe(III) again into Fe (II), which in turn  
40 produces further  $HO^\bullet$  radicals (Eq. 3) and results in a cycle continuously supplying  $HO^\bullet$  until  $H_2O_2$  is  
41 depleted. Shorter wavelengths ( $\lambda \leq 310nm$ ) cause peroxide photolysis (Eq. 4) and the direct production  
42 of extra  $HO^\bullet$ . Therefore, the oxidation rate of photo-Fenton results much higher than that of the Fenton  
43 process.





44 Improved versions of the Fenton process are classified according to their hydroxyl radical production  
45 and include Photo-Fenton, electro-Fenton, sono-Fenton, photo-electro-Fenton, photo-sono-Fenton and  
46 sono-electro-Fenton.

47 This work focuses on the Photo-Fenton process, an effective method that takes place on the presence of  
48 Fenton reagents and UV radiation, including natural sunlight, which has been reported to reduce the  
49 operation cost.

50 The  $HO^{\bullet}$  radical is the key species attacking organic molecules in an efficient but non-selective manner.  
51 However, an unnecessarily high concentration of  $HO^{\bullet}$  (if  $H_2O_2$  is added in excess) can cause  
52 unproductive reactions (Eq. 5-6) downgrading process performance (Tokumura et al., 2011):



53 Using  $H_2O_2$  is essential, but oversupplying is counterproductive. The supply of hydrogen peroxide, as a  
54 means to control the concentration of hydroxyl radicals, is the most important operational parameter for  
55 the photo-Fenton process affecting both reaction outcome and process cost (Ortega-Gomez et al., 2012).  
56 Accordingly, a number of works has been dedicated to determining conditions enhancing process  
57 performance through a sensible hydrogen peroxide supply. Despite the progress reported by recent works  
58 (Yamal-Turbay et al., 2012; Pouran et al., 2015; Wang et al., 2016; Esteves et al., 2018), solutions are  
59 still partial and far from optimal.

60 Most proposals are heuristic strategies that are useful in particular situations, although they that cannot  
61 provide the optimal solution. However, optimization is a systematic strategy leading not to an improved  
62 solution but to the solution for which is proved that no other better solution exists.

---

63 Initially, research sought for adequate concentration ratios of  $H_2O_2$  to contaminant and iron (Pignatello  
64 et al., 2006) in an attempt to minimize the scavenging effect. However, constant ratios may suit steady  
65 operation, but time-varying batch processes (such as these addressed in this work and those usually  
66 reported in the literature –e.g. Pouran et al., 2015) require  $H_2O_2$  supply to be continuously adapted to  
67 maximize the final operation performance. Thus, the real research challenge is the optimization of a  
68 continuous time-dependent  $H_2O_2$  dosage profile.

69 Monteagudo et al. (2009) and Zazo et al. (2009) proved that continuously dosing  $H_2O_2$  along the reaction  
70 time can increase oxidation efficiency beyond that obtained by administering a total dose of  $H_2O_2$  at the  
71 beginning of the reaction (henceforth no dosage).  $H_2O_2$  discretized dosage by splitting the total supply  
72 into several portions and adding them at different times has also been reported to produce improvements  
73 respect no dosage. However, the use of arbitrary time intervals prevents the solutions to be reported as  
74 optimal. Some researchers reported that sequential addition of discrete amounts of  $H_2O_2$  leads to better  
75 results than adding a great initial dose (Chu et al., 2007; Almeida et al., 2015). Other previous works  
76 reported that adding  $H_2O_2$  at a constant rate into the reactor along the reaction time increases the process  
77 efficiency (Monteagudo et al. 2009 Prato-Garcia et al., 2012). However, other researchers have drawn  
78 completely opposite conclusions (Chidambara and Quen, 2005; Zhou et al., 2016). Certainly, this  
79 divergence shows that dosage is still an open issue deserving attention, particularly with regard to a  
80 systematic approach and the standardized comparison of methods and results. Other works have  
81 addressed  $H_2O_2$  dosage as a continuous control problem. Santos-Juanes et al. (2011) used the on-line  
82 monitoring of dissolved oxygen (DO) to regulate the dosage of  $H_2O_2$  and greatly improve the operation  
83 performance. Despite the practical achievement, the strategy relies on the expert setting of an indirect  
84 factor (DO set-point) assumed to reveal the operation performance, and it cannot be proved optimal. A  
85 general systematic strategy based on an accurate statement of an optimization problem is still pending.

86 On the other hand, the optimization of similar problems has been successfully reported, such as the  
87 optimization of batch and fed-batch operations by model-based approaches (Biegler, 2018; Jang et al.,  
88 2016; Nie et al., 2014). The general dynamic optimization problem addressed consists on determining a  
89 control law (the recipe) that drives the process through a feasible trajectory on a continuous time interval  
90 and minimizes a given cost function at the end of the interval. The ordered set of decisions made along  
91 the given time horizon and the practical discrete approximation required by the numerical solution

---

92 approach is in the basis of this work.

93 Nevertheless, for Fenton and photo-Fenton processes, the lack of suitable dynamic models hinders  
94 model-based optimization to a great extent (Qin and Badgwell, 2003; Jung et al., 2015), and the idea of  
95 model-based optimization to determine the best hydrogen peroxide supply profile along a batch run (the  
96 recipe) has been hardly addressed (Audino et al., 2019).

97 Since, the optimization of the operation of the photo-Fenton process, and particularly of the  $H_2O_2$  dosage  
98 problem, is a continuous optimal control problem that should be formulated and addressed as such, this  
99 work uses recipe optimization concepts and a convenient time discretization to propose a practical  
100 methodology for experimentally addressing the optimization of hydrogen peroxide dosage profile. The  
101 adoption of this approach favors the convergence with the model-based optimization approach.

102 The proposed methodology is tested through its application to the remediation of a Paracetamol (PCT)  
103 solution. Furthermore, taking into account that several authors (Prieto-Rodríguez et al., 2011; Ortega-  
104 Gómez et al., 2012) have proposed using the variation of the concentration of dissolved oxygen (DO) for  
105 tactically adjusting hydrogen peroxide supply, this work also measures and discusses the response in DO  
106 concentration in order to provide deeper insight into the nature of the process.

## 107 **2. Dosage modelling and problem formulation**

108 Dosing hydrogen peroxide in batch Fenton and Photo-Fenton processes is a decision-making problem.  
109 Once admitted the existence of dosage alternatives, the problem consists in selecting a feasible alternative  
110 satisfying the given constraints and, eventually, the alternative producing the best outcome, the so-called  
111 optimal decision. Heuristic rules (tactical step moves based on local information) provide fast and  
112 practical decision-making support, but they do not drive to the optimal decision (the full set of moves for  
113 which the inexistence of any better alternatives for the complete problem can be proved), and they lean  
114 towards concealing misconceptions (mistaking the goal). Conversely, optimization techniques seek for  
115 the optimum at the expense of analyzing and quantitatively assessing all the alternatives (explicitly or  
116 implicitly, in the case of efficient search methods).

117 This work addresses the optimization of hydrogen peroxide dosage in batch Fenton and Photo-Fenton

---

118 processes. Accordingly, this work undertakes a systematic problem analysis and formulation (including  
119 declared assumptions and simplifications) that contributes a methodological approach aimed at stirring  
120 discussion and further research. Next, this section sets system boundaries and operational constraints,  
121 offers the definition of an objective function quantitatively assessing the outcomes of the decisions, and  
122 proposes a search method. The search can be performed using a mathematical abstraction accurately  
123 representing the system under study, or experimentally (Box et al., 2005). Lacking convenient kinetic  
124 models, this work undertakes an experimental approach, which is more expensive but consistent with the  
125 model-based optimization approach used for solving similar dynamic optimization problems in industrial  
126 applications (Biegler, 2018; Jang et al., 2016; Nie et al., 2014).

127 A first assumption is batch operation. While continuous operation might be the choice for industrial  
128 solutions, most of the academic research focuses on batch assays (Pouran et al. 2015), probably because  
129 of the operational costs. Dosage in batch processing poses a dynamic optimization problem: determine  
130 the dosage level at each infinitesimal time interval (the trajectory of the control action) that minimizes  
131 (or maximizes) a given integral function at the end of a given finite interval.

132 The discrete approximation applied in the numerical solution of the model-based approach is for the  
133 experimental approach not only inevitable, but required of additional simplification.

## 134 **2.1. Problem formulation**

135 The proposed dosage model assumes a single objective  $J$  to be minimized by the operation of a Fenton  
136 or photo-Fenton reactor.  $J$  is the outcome of the operation after some reaction time  $T$  and after the addition  
137 of some total amount  $A$  of reactant (e.g. volume of  $H_2O_2$  solution). As Fenton and photo-Fenton processes  
138 are mostly operated in batch, this outcome has to be a fix value that describes the performance of the  
139 process, such as an economic indicator or the final concentration of a given species. Likewise, the method  
140 could be applied to continuous processes by selecting a derivative (e.g. reaction rate) as an indicator.

141

142 **Fig 1.** General discretization of the dosage profile. Theoretical framework.

143 A fraction  $f$  ( $0 \leq f \leq 1$ ) of this total amount  $A$  can be dosed following different schemes during the

144 time horizon, while the remaining fraction ( $A_0 = (1 - f) \cdot A$ ) is assumed to be added at once at the  
 145 very beginning. Assume the reaction time  $T$  is discretized in  $i = 1, 2, 3 \dots N$  time slots, each of duration  
 146  $\Delta t = T/N$ , and  $L \in N$  dosage levels as represented in Figure 1 (in the limit,  $N, L \rightarrow \infty$ , this discretization  
 147 allows considering time and supply as a continuous decision variables). Hence, for each time slot  $i$  the  
 148 dosage level  $x_i \in \{0, 1, 2 \dots, L\}$  needs to be determined so that the balance and flow constraints on  $A$  are  
 149 satisfied and the outcome  $J = f(\mathbf{x}, f, A, T)$  is minimized (Eq. 7).

150 The formulation of the dosage model includes the integral of dosage bits ( $X$ , Eq. 8) that determines the  
 151 incremental addition at each time interval ( $\Delta A_i$ , Eq. 9). Hence, Eq. 10 allows determining and bounding  
 152 (e.g. pumping capacity) the corresponding dosage flows  $F_i$  for each time slot.

$$J = f(\mathbf{x}, f, A, T) \tag{Eq. 7}$$

s.t.

$$X = \sum_i x_i \tag{Eq. 8}$$

$$\Delta A_i = \left( \frac{f \cdot A}{X} \right) \cdot x_i \quad \forall i \tag{Eq. 9}$$

$$F^{min} \leq F_i = \frac{\Delta A_i}{\Delta t} \leq F^{max} \quad \forall i \tag{Eq. 10}$$

153 The outcome  $J = f(\mathbf{x}, f, A, T)$  could be inexpensively determined through a convenient mathematical  
 154 model  $f$ , if available, or experimentally. This work relies on the experimental measurement of the  
 155 objective function  $J$  for exploring and assessing the alternatives and detecting the best one. The infinite  
 156 solution space and the too expensive experimental search requires some further assumptions to positively  
 157 address such identification.

158 In regard of decision variables, the following experimental work assumes a given time horizon  $T$  (thus,  
 159 excluding the minimization of the reaction time) and disregards the consideration of any initial amount  
 160 of reactant ( $f = 1 \rightarrow A_0 = 0$ ). The total amount  $A$  will be also assumed fixed, but some assays will be

---

161 presented providing insight and discussion concerning the stoichiometric amount. Thus, the general  
162 dosage problem presented is addressed in a reduced form consisting in determining the maximum  
163 distance we can drive on this road given this time and this amount of fuel; lacking a map of the road, the  
164 problem is addressed by methodically planning and executing a series of runs.

165 In regard of the modelling parameters  $N$  and  $\Delta t$ , this work proposes a first discretization aimed at  
166 achieving the practicality required by the evaluation of the methodology. Besides, the work also explores  
167 an alternative in order to offer data and discussion on the effect and sensitivity of such parameter values.  
168 Other implementations are deemed for future research and, in the same way that further problem  
169 extensions, may be envisaged stemming from the proposed formulation.

## 170 **2.2. Design of Experiments**

171 While this problem statement defines a comprehensive theoretical framework to address the dosage  
172 problem (consistent with the numerical solution of the optimization problem, if a reliable process model  
173 was available), it also defines an unaffordable solution space of  $(L + 1)^N$  experimental assays. Thus, this  
174 work also analyses the practical ways to address the corresponding design of experiments by identifying  
175 and removing unrealistic solutions. Further simplifications are discussed in regard to the granularity  
176 adopted and the practicality of the solutions attained.

177 A first issue to decide is the objective function. As stated in the previous section, it has to be a final  
178 indicator of the performance of the process of a batch process. Among other complex alternatives  
179 (economic and/or environmental impacts), this work sets the outcome to be minimized as the Total  
180 Organic Carbon (TOC) concentration measured at the end of a given reaction time (i.e.  $[TOC]_T$ ). The  
181 particular choice of TOC at the end of a time horizon, is commonly used by many authors, including  
182 those addressing hydrogen peroxide dosage (Herney-Ramirez et al., 2010; Pouran et al., 2015). TOC is  
183 a valuable index of water quality as it reveals the extent of mineralization of mother starting (pollutants  
184 plus the formed intermediates). The reagent to be dosed is Hydrogen peroxide, and its amount  $A$  is  
185 defined in terms of volume of water solution (reagent-grade, 33%  $w/v$ ).

186 Moreover, the dosage level is simplified to a binary decision for each time slot  $i$ ; thus,  $x_i \in \{0,1\}$  (Figure



---

187 2A). Further considerations include setting  $x_i = 1$  for the first slot (since no reaction is expected  
188 otherwise) and setting  $x_i = 0$  for the last slots in the series (since the reaction is expected to continue for  
189 a while without further dosage) as represented in Figure 2B. These are practical assumptions (e.g., the  
190 first time slot could have no duration, in order to consider an initial immediate addition of reactant), and  
191 they can be revised later on depending on the results.

192 **Fig 2.** Discretization of the dosage profile (A) considering binary decisions and (B) fixing first and last  
193 time slots.

194 The time horizon  $T$  is set to 120 minutes. This reaction time is fixed according to the preliminary  
195 experiments using a single  $\text{H}_2\text{O}_2$  addition. The monitoring of the  $\text{H}_2\text{O}_2$  concentration (Figure 3B) shows  
196 that the stoichiometric amount of  $\text{H}_2\text{O}_2$  is almost exhausted after 120 minutes. Thus, the slot size  $\Delta t$  is  
197 the last decision to be made. It is set to 15 min, which leads to  $N = 8$  and  $2^N = 256$  alternatives to be  
198 explored. Since there are four slots assumed to be determined beforehand (the first and the last three) the  
199 solution space is again reduced and only  $2^{N-4} = 16$  assays are finally planned. For the sake of  
200 illustration, assume a finer partition given by a  $\Delta t$  value reduced to 5 min (only to one third). Hence,  
201  $N = 24$  and the alternatives to be explored would be  $2^{N-4} = 1048576$ , which is experimentally  
202 unaffordable.

203 **Table 1.** Design of experiments. The dosage level (0, 1) is given for the eight time slots S1 to S8; the  
204 preset values for slots S1, S6, S7 and S8 are shadowed. The reactant fraction to be dosed at each active  
205 slot is also given.

### 206 **3. Materials and methods**

207 Paracetamol (98% purity) was purchased from Sigma-Aldrich. Hydrogen peroxide (reagent-grade, 33%  
208  $w/v$ ) was purchased from Panreac. Heptahydrate ferrous sulfate ( $\text{FeSO}_4 \cdot 7\text{H}_2\text{O}$ ) used as the ferrous ion  
209 was acquired from Merck. Sulfuric acid ( $\text{H}_2\text{SO}_4$  95%) from Fisher was used for pH adjustment.  
210 Ammonium metavanadate ( $\text{NH}_4\text{VO}_3$  98.5%) was used for  $\text{H}_2\text{O}_2$  measurement. HPLC gradient grade  
211 Methanol (MeOH) was acquired from J.T. Baker Inc. and ultra-pure solvents (Milli-Q<sup>®</sup> water) were  
212 prepared for HPLC mobile phase. Distilled water was used as water matrix for solution preparation.

---

213 The experimental setup is an automated photochemical pilot plant. The reaction system includes a 13.5  
214 L glass jacketed reservoir tank and a 1.5 L glass tubular photo-reactor (10 % of the total volume) with an  
215 irradiated height of 130 mm). The radiation source is a Philips Actinic BL TL 36 W/10 1SL lamp (UVA-  
216 UVB), the incident photon power,  $E = 3.36 \times 10^{-4}$  Einstein  $\text{min}^{-1}$  (300 and 420 nm) was measured using  
217 potassium ferrioxalate actinometry. The recirculation fluid is driving through the reservoir tank and the  
218 photo-reactor by a centrifugal pump (Iwaki Magnet Pump, MD-30RZ-220, 1-16HP-220V). Sensors are  
219 also equipped for measuring pH (Hamilton Polilyte HTVP 120), intensity of UV radiation on the external  
220 surface (Sglux UV\_Surface\_A\_4-20mA\_cable), temperature and dissolved oxygen (Hamilton Oxysens).  
221 H<sub>2</sub>O<sub>2</sub> dosage is automatically performed through a peristaltic pump (Watson Marlow, OEM 313 24V)  
222 and a PLC (Siemens SIMATIC S7-1200) managed by the plant SCADA system (InTouchR<sup>®</sup> software).

### 223 **3.1. Analytical methods**

224 Total organic carbon (TOC) concentration was determined with a TOC (TOC-VCSH/CSN Shimadzu;  
225 Kyoto, Japan) analyzer. Samples were taken every 15 min and kept in the ice to slow down further  
226 oxidation.

227 PCT concentration was measured via HPLC Agilent 1200 series (Agilent Technologies) with UV-DAD  
228 array detector. The chromatographic column was a 5  $\mu\text{m}$  4.6 mm $\times$ 150 mm Akady Ultrabase C-18. 20  $\mu\text{l}$   
229 samples, the detection wavelength was set to 243 nm and the temperature was fixed to 25  $^{\circ}\text{C}$ . The eluent  
230 was a mixture of methanol and water (25:75) with a flow rate of 0.4 mL  $\text{min}^{-1}$  (Yamal-Turbay et al.,  
231 2015), retention time was 7.3 min under these conditions. Samples were taken at different times and were  
232 previously treated with methanol (in proportion 50:50) in order to stop further degradation of PCT.

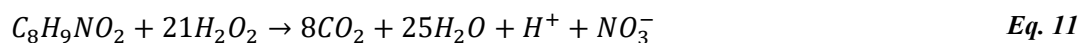
233 H<sub>2</sub>O<sub>2</sub> concentration was measured by using the spectrophotometric method (Nogueira et al., 2005). The  
234 absorption at 450 nm was detected via a U-2001 UV-vis spectrophotometer (Hitachi, Tokyo, Japan).

### 235 **3.2. Experimental procedure**

236 The conditions of the photo-Fenton experiments were: pH adjusted to  $2.8 \pm 0.2$  using H<sub>2</sub>SO<sub>4</sub> and  
237 temperature 26-28  $^{\circ}\text{C}$ . The initial solution in the reactor was prepared with 15 L of distilled water and  
238 0.6122 g of model pollutant PCT and 0.7468 g of FeSO<sub>4</sub>·7H<sub>2</sub>O (40 mg L<sup>-1</sup> PCT and 10 mg L<sup>-1</sup> Fe(II)).

---

239 The total amount of hydrogen peroxide to be dosed, A, is set to be the stoichiometric concentration  
240 (considering H<sub>2</sub>O<sub>2</sub> as the only oxidant in the media, Eq. 11), S, for the given amount of PCT: this is 9.545  
241 g (8.5909 mL of solution 33% w/v), which corresponds to a concentration of 189 mg L<sup>-1</sup> (S).



242

243 **Table 2.** List of assays carried out using 40 mg L<sup>-1</sup> PCT and 189 mg L<sup>-1</sup> of H<sub>2</sub>O<sub>2</sub> (the corresponding to  
244 the stoichiometric amount, S).

245 The UV light was switched on as soon as FeSO<sub>4</sub>·7H<sub>2</sub>O and PCT were added in order to guarantee its  
246 stabilization. The execution of the dosage program started 10 min after to ensure perfect mixing. The  
247 dosage of the H<sub>2</sub>O<sub>2</sub> solution followed the specific values set for experiment and shown in Table 2, and  
248 the specific dosage time intervals 0, 15, 30, 45, 60 min. All experiments were repeated twice, the average  
249 values were obtained to exhibit the TOC conversion, PCT degradation, and H<sub>2</sub>O<sub>2</sub> evolution.

## 250 4. Results and discussion

### 251 4.1 Preliminary results

252 Preliminary tests were performed to a 40 mg L<sup>-1</sup> PCT sample to identify the contribution to the  
253 mineralization of PCT of factors such as reagent and irradiation. The tests (Figure 3) were performed at  
254 pH= 2.8 ± 0.2 and T = 26-28 °C, and the loads of the Fenton reagents were [Fe(II)] = 10 mg L<sup>-1</sup> and  
255 [H<sub>2</sub>O<sub>2</sub>] = 189 mg L<sup>-1</sup> (corresponding to the stoichiometric amount, S).

256 **Fig 3.** (A) Evolution of TOC concentrations upon blank assays. (B) Comparison of Fenton and photo-  
257 Fenton process: evolution of TOC and H<sub>2</sub>O<sub>2</sub> concentrations

258

259 The results of these tests can be summarized as follows:

- 
- 260 • Negligible mineralization was attained in all the blank tests (Figure 3A), even in the assays with sole  
261 H<sub>2</sub>O<sub>2</sub>, sole irradiation, and the combination of both.
- 262 • The comparison between the results of the Fenton and the photo-Fenton processes (Figure 3B) shows  
263 that UV irradiation significantly enhanced the conversion attained. This is due to already mentioned  
264 role of UV-vis light, which increases the mineralization from 23.3 % to 57.15 %.

265 Once demonstrated the higher mineralization capacity of the photo-Fenton process, the next step is  
266 studying the effect of H<sub>2</sub>O<sub>2</sub> dosage on the performance of photo-Fenton processes aimed at determining  
267 the best dosage scheme.

## 268 4.2 Base case

269 The 16 dosage schemes planned (Table 2) were first performed for 40 mg L<sup>-1</sup> PCT and the stoichiometric  
270 amount of H<sub>2</sub>O<sub>2</sub> (S, 189 mg L<sup>-1</sup>) to be dosed along a time horizon of two hours ( $T=120$  min). Clearly,  
271 the stoichiometric amount cannot be expected to achieve total mineralization. However, it is useful for  
272 providing reference results for quantitative comparison.

273 Additional measurements were taken beyond this time horizon for TOC (up to 240 min, in order not to  
274 miss further reaction progress), while measurements for PCT were interrupted earlier, as they fell below  
275 the detection limits of the analytical techniques.

276 Table 2 presents the assays using the binary code, which clearly express the dosage profile. The label  
277 NO\_DOSAGE refers to the assay for which the same total amount of H<sub>2</sub>O<sub>2</sub> was supplied all at once at  
278 the beginning. All these assays were repeated twice and variability of TOC concentration was found to  
279 be low (below 4 %). Therefore, from here on, only the average of all these repeated measurements is  
280 presented.

281 All these assays show that PCT completely reacts within the first 45 min. However, the time required for  
282 PCT concentration to drop below the detection limits depends on the number and size of the dosing bits  
283 (the distribution of the H<sub>2</sub>O<sub>2</sub> supply along the time). For a first assay, G1 = {0000}, no presence of PCT  
284 is detected after 15 min; for the group of assays G2 = {0001, 0010, 0100, 1000}, no presence of PCT is  
285 detected after 25 min; for the groups G3 = {0011, 0101, 0110, 1100, 1001, 1010}, G4 = {0111, 1011,

---

286 1101, 1110}, and  $G5 = \{1111\}$ , tending to continuous supply, the time spans from 25 to 45 min.

287 The higher the number of the dosing bits (the lower the  $H_2O_2$  amount added in each time slot), the slower  
288 the PCT elimination. Figure 4 shows the hydrogen peroxide present in the system for each group.  
289 NO\_DOSAGE is the assay producing the PCT fastest elimination, while the rest G1 (0.573 mL/min at  
290 first dosing interval), G2 (0.286 mL/min at each dosing interval), G3 (0.286 mL/min), G4 (0.286  
291 mL/min), and G5 (0.286 mL/min), result increasingly slower. Thus, these results allow concluding that,  
292 only in regard to PCT removal, the most concentrated reactants at the beginning, the best performance,  
293 which suggests that the scavenging effect should be expected later and involved with intermediate  
294 products.

295 **Fig 4.** Hydrogen peroxide profiles (A) all assays (B) with two doses, G2 (C) with three doses, G3 (D)  
296 with four and five doses, G4 and G5.

297 The evolution of the concentration of  $H_2O_2$  is studied and presented in the above set of figures (Figure  
298 4). The dashed line plotting the evolution when  $H_2O_2$  is added all at once at the beginning  
299 (NO\_DOSAGE) reveals that the same amount,  $S$ , of  $H_2O_2$  is consumed much faster and exhausted by  
300 135 min. On the other hand, other dosing schemes produce  $H_2O_2$  profiles that span longer and may exhibit  
301 peaks and valleys (Figures 4B and 4C), which may be interpreted as a gap between supply and demand.  
302 This seems not the case for the more continuous dosage given by G4 and G5 (Figure 4D), although this  
303 cannot be deemed as the most efficient.

304 The identification of the best protocol is given by Figure 5 (according to the objective function set to be  
305 minimized,  $J = [TOC]_{120}$ ) and is revealed to be 1000 (61.90% conversion) and 0000 (61.70%  
306 conversion), which is an improvement of 4.75 percent points NO DOSAGE (57.15% conversion). This  
307 may seem a minor improvement, but it can be much more significant in regard of process economy.  
308 Despite this numerical value, the improvement is shown to be systematically determined by the dosage  
309 modelling proposed and the experimental design derived accordingly. On the other hand, 0011 and 0001  
310 are revealed to have worse performance than NO\_DOSAGE; indeed, this can be attributed to a demand  
311 of  $H_2O_2$  that is attended too late (although it can be expected to have an effect beyond  $T = 120$  min). The  
312 comparative details of these extreme situations are given in Figures 6.

---

313 **Fig 5.** TOC conversion after 120 min under photo-Fenton treatment. The total amount of hydrogen  
314 peroxide added during 120 min is the stoichiometric quantity. Table 2 summarize the dosing strategies.

315 **Fig 6.** Hydrogen peroxide inlet flow, measured hydrogen peroxide concentration, and reference  
316 concentration (the one that would result from the addition to a non-reacting system): (A) 0001 (the  
317 worse scheme) (B) and 1000 (the best scheme)

318 Finally, the evolution of dissolved oxygen concentration (DO) is also monitored for tactical purposes  
319 and for a more complete interpretation of the underlying nature of the process (Figure 7). DO level has  
320 been interpreted as a practical indicator of process efficiency (Santos-Juanes et al., 2011). Thus, while  
321 low DO levels might indicate the need for more H<sub>2</sub>O<sub>2</sub>, the rising of DO might indicate an unproductive  
322 decomposition of hydrogen peroxide that should be avoided.

323 **Fig 7.** Evolution of DO level for assays NO\_DOSAGE, 1000 and 0001.

324 Accordingly, Figure 7 might suggest that NO\_DOSAGE, providing more moderate peaks and valleys,  
325 should produce the best performance, which is obtained by 1000. Conversely, both assays 1000 and  
326 0001, experience a smoother start. This shows that, although DO is a practical indicator, the relationship  
327 between this indicator and the performance (minimizing TOC, or cost, or any other objective function  
328 that may be proposed) is not direct and deserves attention beyond this first experimental design proposed  
329 to illustrate the methodology.

330 On one hand, the aggregate and indirect information provided by the DO level at time  $t < T$  cannot  
331 anticipate the outcome of the process at time  $T$ , and it cannot drive decisions to an optimal outcome. On  
332 the other hand, the change in the DO level (its derivative at time  $t < T$ ) may provide local information  
333 that could eventually drive tactical decisions (adding H<sub>2</sub>O<sub>2</sub>). In this regard, the change of the DO level is  
334 a robust measurement, since it is relative and insensitive to offsets and interferences caused by side  
335 reactions and intermediate products. However, developing an accurate correlation of the level of  
336 dissolved oxygen with these factors, including delays due to the diffusion of the dissolved oxygen, is  
337 complex challenge out of the scope of this paper.

### 338 **4.3 Extended cases**

339 This section investigates some of the implicit assumptions accepted up to this point.

---

340 The proposed dosage model assumes a general single objective  $J$  that for the base case was TOC  
341 concentration after 120 min:  $J = [TOC]_{120}$ . In addition to this objective function, the total amount of  
342 hydrogen peroxide to be added was set to be the stoichiometric ( $A = S$ ) and the initial amount was set to  
343 be zero ( $A_0 = 0$ ). Finally yet importantly, the intervals were arbitrarily fixed to 15 min. Such decisions  
344 are not inherent to the methodology and they could be controlled to achieve better performance.

### 345 **4.3.1 Objective function**

346 A first extension in the objective function consists in changing the reaction time. Thus, a new set of  
347 assays was performed for a time horizon of four hours ( $T= 240$  min), and the conversions obtained for  
348  $J = [TOC]_{240}$  were ranked and compared with those in the previous section. For this extended reaction  
349 span, the best conversion was 6 percent points higher than that obtained without dosage.

350 A new objective function can also be proposed by considering the reverse approach: the earliest time to  
351 achieve a specified conversion. Given the same conversions, such a time is obtained by the linear  
352 interpolation of the measured values. For instance, the time required for reaching 70% conversion show  
353 that while 240 min are required if no dosage is applied, only 167 min (73 min less) are required for the  
354 most efficient dosage protocol (1000).

### 355 **4.3.2 Hydrogen peroxide amount**

356 The first set of assays were planned with a total amount of hydrogen peroxide,  $A$ , equal to the  
357 stoichiometric amount. This is an assumption based on the idea that an ideal dosage protocol should exist  
358 that would cause no hydrogen peroxide dissipation in any unproductive reaction. However, more than  
359 the stoichiometric amount could achieve better performance. Therefore, this sub-section explores the  
360 effect of different amounts of hydrogen peroxide. Certainly, the idea of  $A$  as decision variable instead of  
361 a fixed parameter is implicit in the problem formulation (Eq.7), but attempting such an extended  
362 optimization problem is out of the scope of this work.

363 In Figure 8 and from this point on, experiments are codified using the same ID (bin) from Table 2, plus  
364 the amount of hydrogen peroxide referred to the stoichiometric amount,  $S$ , specifically  $S$  (189 mg L<sup>-1</sup>),  
365  $1.2S$  (226.8 mg L<sup>-1</sup>), and  $2S$  (378 mg L<sup>-1</sup>).

---

366 **Fig 8.** Evolution of the TOC concentration (normalized) for the assays S\_NO DOSAGE, 2S\_NO  
367 DOSAGE and S\_1000\_08.

368 Figure 8 shows how the best dosage protocol (S\_1000\_08) reaches similar mineralization value (68 %,   
369 150 min) than NO\_DOSAGE assay with double hydrogen peroxide amount (2S\_No Dosage). The   
370 methodology allows to save half of the hydrogen peroxide amount.

### 371 **4.3.3 Hydrogen peroxide initial amount ( $A_0$ )**

372 DO performance allows analyzing the appropriate initial amount of hydrogen peroxide in order to avoid   
373 the marked decrease in oxygen consumption general produced in dosage assays at early stages of the   
374 oxidation process. Towards this end, a new set of experiments were performed to obtain a new set of   
375 outcomes at 120 min for different initial amounts of hydrogen peroxide (Table 3).

376 **Table 3.** TOC conversions obtained at 120 min with different hydrogen peroxide amounts (A) and initial   
377 amounts ( $A_0$ ) and the conversion obtained. The stoichiometric amount (S) is  $189 \text{ mg}\cdot\text{L}^{-1}$ .

378 **Fig 9.** Evolution of the DO concentration for the assays given in Table 3.

379 Figure 9 presents the corresponding DO profiles. For this particular case (the dynamics of the photo-   
380 Fenton process are strongly dependent on the nature of the organic matter to be degraded), 0.2S obtain   
381 flatter DO performance at the first time reactions.

382 It is worth noting that DO levels attain levels far beyond saturation. As commented previously, DO   
383 absolute values usually depend on many factors (pressure, temperature, salinity...) in addition to those   
384 specifically provided by the Photo-Fenton reacting environment (intermediates, radicals...). Other works   
385 monitoring DO in Photo-Fenton processes also report similar values noticeably exceeding DO saturation   
386 (Santos-Juanes et al. 2011, Ortega-Gómez et al. 2012). This works also propose the reactions producing   
387  $\text{O}_2$ . Another important factor to observe is process dynamics, and the accumulation caused by  $\text{O}_2$    
388 production rates larger than the oxygen diffusion rate. This effect is included in the model introduced by   
389 Cabrera-Reina et al. (2012).

### 390 **4.3.4 Time discretization**



---

391 Finally, time discretization is addressed in this last experiment. Related to the interval time slots only  
392 two options were tested (from 15 to 5 min) the results (Figure 10) evidence a clear effect of this  
393 parameter. Further studies are required in order to optimize it.

394 **Fig 10.** Evolution of the DO concentration for the assays with different time discretization.

395 All these results are exploring different variations of the initial experimental design open promising  
396 research lines. The development of a methodology for determining the best dosage protocol for the photo-  
397 Fenton process deserves the attention of future work.

## 398 **5. Conclusions**

399 This work presents a comprehensive theoretical framework to address the problem of hydrogen peroxide  
400 dosage for Fenton and photo-Fenton processes in a systematic way. The work proposes a problem  
401 formulation that provides a new insight into the nature of the decision-making problem, and allows  
402 further discussion of tactical and strategic solution approaches. The framework is based on the underlying  
403 dynamic optimization essence of the problem. A natural discretization scheme is adopted to develop a  
404 new dosage model for which advantages and limitations are discussed. With the aim to overcome the  
405 current lack of models that provide model-based solution approaches, this work is expected to shed new  
406 light to the dosage problem by addressing it from an experimental approach.

407 A practical experimental design is proposed and assumptions are made to reduce the dosage level to a  
408 set of binary decisions, as well as fixing reaction time and the total amount of hydrogen peroxide. This  
409 experimental approach is consistent with the model-based optimization approach and sets a framework  
410 to further develop and validate a mathematical model for the dosage. Accordingly, a complete set of  
411 dosage schemes were implemented and assessed for the study of paracetamol (PCT) degradation.

412 The quantitative results obtained allow sorting out the alternatives and identifying the best dosage profile,  
413 which increases TOC conversion by 4.75 percent points (after 120 minute). Additionally, complementary  
414 measurements allowed to further discuss the complex nature of the different interconnected processes  
415 causing such an outcome. All the treatments under study attained the total elimination of initial PCT  
416 within a minimum time of 7 min and maximum time of 45 min (over a time horizon of 120 min). The

---

417 measurement of the corresponding DO concentration allowed concluding that no simple relation seems  
418 to exist between the observed DO values and the final outcome of the process at the end of the time  
419 horizon (e.g.  $[TOC]_T$ ). However, the study of DO profiles in parallel to the corresponding dosage profiles  
420 might provide meaningful and practical correlations for tactical purposes.

421 Other objectives and configurations were studied to envisage new aspects to be explored. Thus, decisions  
422 not inherent to the methodology (the total amount of hydrogen peroxide to be added, the initial amount  
423 of hydrogen peroxide, the intervals time slots) were modified and tested to achieve better system  
424 performance. When the goal was to minimize TOC concentration after 240 min ( $J = [TOC]_{240}$ ), the  
425 mineralization was further improved (by to 6 percent points) with the same amount of hydrogen peroxide.

426 Conversely, attending the inverse objective (the earliest time required to meet a certain TOC value) led  
427 to determining that the same mineralization was achieved within 167 min or 240 min, depending on the  
428 dosage protocol. The effect of an initial amount of hydrogen peroxide was also addressed and studied.  
429 When the monitoring of the DO levels was included, the marked decrease in oxygen consumption  
430 produced at early stages of the oxidation process was shown to be moderated. Finally, changing time  
431 discretization (from 15 to 5 min) revealed that this is a very influencing aspect deserving further studies  
432 and that future work should continue progressing towards a model-based optimal control of photo-Fenton  
433 processes.

## 434 **Notation**

435 **Table 4.** Notation for the mathematical model.

436

## 437 **Acknowledgements**

438 This work was supported by the Spanish "Ministerio de Economía, Industria y Competitividad  
439 (MINECO)" and the European Regional Development Fund, both funding the research Project AIMS  
440 (DPI2017-87435-R). Yu Xiangwei particularly acknowledges the State Scholarship Fund of China  
441 Scholarship Council (No. 201706950041). Ana Somoza-Tornos thankfully acknowledges financial

---

442 support received from the Spanish Ministry of Education, Culture and Sport (Ayuda para la Formación  
443 de Profesorado Universitario - FPU15/02932).

444

---

## 445 **References**

- 446 Almeida, C. V. D. S., Macedo, M. S., Eguiluz, K. I. B., Salazar-Banda, G. R., Queissada, D. D., 2015.  
447 Indanthrene Blue Dye Degradation by UV/H<sub>2</sub>O<sub>2</sub> Process: H<sub>2</sub>O<sub>2</sub> as a Single or Fractioned  
448 Aliquot? *Environ. Eng. Sci.* 32, 930-937. doi:10.1089/ees.2015.0171.
- 449 Audino, F., Companyà, G., Pérez-Moya, M., Espuña, A., Graells, M., 2019. Systematic optimization  
450 approach for the efficient management of the photo-Fenton treatment process. *Sci. Total*  
451 *Environ.* 646, 902-913. doi:10.1016/j.scitotenv.2018.07.057.
- 452 Biegler, L.T., 2018. Advanced optimization strategies for integrated dynamic process operations. *Comp.*  
453 *Chem. Engng.* 114, 9, 3-13. doi:10.1016/j.compchemeng.2017.10.016.
- 454 Box, G. E. P., Hunter, J.S., Hunter, W.G., 2005. *Statistics for Experimenters: Design Innovation and*  
455 *Discovery*, USA, NY, New York:Wiley-Interscience.
- 456 Cabrera-Reina, A., Santos-Juanes, L., García, J.L., Casas, J.L., Sánchez, J.S., 2012. Modelling photo-  
457 Fenton process for organic matter mineralization, hydrogen peroxide consumption and  
458 dissolved oxygen evolution. *Appl. Catal. B Environ.*, 119-120,132–138.  
459 doi:10.1016/j.apcatb.2012.02.021
- 460 Chu, W., Chan, K. H., Kwan, C. Y., Choi, K. Y., 2007. Degradation of atrazine by modified stepwise-  
461 Fenton's processes. *Chemosphere* 67, 755-761. doi:10.1016/j.chemosphere.2006.10.039.
- 462 Chidambara Raj, C. B., Quen, H. L., 2005. Advanced oxidation processes for wastewater treatment:  
463 Optimization of UV/H<sub>2</sub>O<sub>2</sub> process through a statistical technique. *Chem. Eng. Sci.* 60, 5305-  
464 5311. doi:10.1016/j.ces.2005.03.065.
- 465 Esteves, B. M., Rodrigues, C. S., Madeira, L. M., 2018. Synthetic olive mill wastewater treatment by  
466 Fenton's process in batch and continuous reactors operation. *Environ. Sci. Pollut. Res.* 25,  
467 34826–34838. doi:10.1007/s11356-017-0532-y.
- 468 Herney-Ramirez J., Vicente M. A., Madeira, L. M., 2010. Heterogeneous photo-Fenton oxidation with  
469 pillared clay-based catalysts for wastewater treatment: A review, *Appl. Catal. B: Environ.*, 98,

---

470 10-26. doi:10.1016/j.apcatb.2010.05.004

471 Jang H., Lee J.H., Biegler L.T., 2016. A robust NMPC scheme for semi-batch polymerization reactors.  
472 IFAC-PapersOnLine 49, 37-42. doi:10.1016/j.ifacol.2016.07.213.

473 Jung, T. Y., Nie, Y., Lee, J. H., Biegler, L. T., 2015. Model-based on-Line optimization framework for  
474 semi-batch polymerization reactors. IFAC-PapersOnLine. 48, 164-169.  
475 doi:10.1016/j.ifacol.2015.08.175.

476 Monteagudo, J. M., Durán, A., San Martín, I., Aguirre, M., 2009. Effect of continuous addition of H<sub>2</sub>O<sub>2</sub>  
477 and air injection on ferrioxalate-assisted solar photo-Fenton degradation of Orange II. Appl.  
478 Catal. B 89, 510-518. doi:10.1016/j.apcatb.2009.01.008.

479 Nie, Y., Biegler, L. T., Villa, C. M., Wassick, J. M., 2014. Discrete time formulation for the integration  
480 of scheduling and dynamic optimization. Ind. Eng. Chem. Res. 54, 4303-4315.  
481 doi:10.1021/ie502960p.

482 Nogueira, R. F. P., Oliveira, M. C., Paterlini, W. C., 2005. Simple and fast spectrophotometric  
483 determination of H<sub>2</sub>O<sub>2</sub> in photo-Fenton reactions using metavanadate. Talanta. 66, 86-91.  
484 doi:10.1016/j.talanta.2004.10.001.

485 Ortega-Gómez, E., Úbeda, J. M., Hervás, J. Á., López, J. C., Jordá, L. S. J., Pérez, J. S., 2012. Automatic  
486 dosage of hydrogen peroxide in solar photo-Fenton plants: development of a control strategy  
487 for efficiency enhancement. J. Hazard. Mater. 237, 223-230.  
488 doi:10.1016/j.jhazmat.2012.08.031.

489 Pignatello, J. J., Oliveros, E., MacKay, A., 2006. Advanced oxidation processes for organic contaminant  
490 destruction based on the Fenton reaction and related chemistry. Crit Rev Environ Sci Technol  
491 36, 1-84. doi:10.1080/10643380500326564

492 Pouran, S. R., Aziz, A. A., Daud, W. M. A. W., 2015. Review on the main advances in photo-Fenton  
493 oxidation system for recalcitrant wastewaters. J Ind Eng Chem 21, 53-69.  
494 doi:10.1016/j.jiec.2014.05.005.

---

495 Prato-García, D., Buitrón, G., 2012. Evaluation of three reagent dosing strategies in a photo-Fenton  
496 process for the decolorization of azo dye mixtures. *J. Hazard. Mater.*, 217–218, 293-300.  
497 doi:10.1016/j.jhazmat.2012.03.036

498 Prieto-Rodríguez, L., Oller, I., Zapata, A., Agüera, A., Malato, S., 2011. Hydrogen peroxide automatic  
499 dosing based on dissolved oxygen concentration during solar photo-Fenton. *Catal. Today* 161,  
500 247-254. doi:10.1016/j.cattod.2010.11.017.

501 Qin, S. J., Badgwell, T. A., 2003. A survey of industrial model predictive control technology. *Control.*  
502 *Eng. Pract.* 11, 733-764. doi:10.1016/s0967-0661(02)00186-7.

503 Santos-Juanes, L., Sánchez, J. G., López, J. C., Oller, I., Malato, S., Pérez, J. S., 2011. Dissolved oxygen  
504 concentration: A key parameter in monitoring the photo-Fenton process. *Appl. Catal. B* 104,  
505 316-323. doi:10.1016/j.apcatb.2011.03.013.

506 Tokumura, M., Morito, R., Hatayama, R., Kawase, Y., 2011. Iron redox cycling in hydroxyl radical  
507 generation during the photo-Fenton oxidative degradation: Dynamic change of hydroxyl radical  
508 concentration. *Appl. Catal. B* 106, 565-576. doi:10.1016/j.apcatb.2011.06.017.

509 Wang, N., Zheng, T., Zhang, G., Wang, P., 2016. A review on Fenton-like processes for organic  
510 wastewater treatment. *J. Environ. Chem. Eng.* 4, 762-787. doi:10.1016/j.jece.2015.12.016.

511 Yamal-Turbay, E., Graells, M., Pérez-Moya, M., 2012. Systematic assessment of the influence of  
512 hydrogen peroxide dosage on caffeine degradation by the photo-Fenton process. *Ind. Eng.*  
513 *Chem. Res.* 51, 4770-4778. doi:10.1021/ie202256k.

514 Yamal-Turbay, E., Ortega, E., Conte, L. O., Graells, M., Mansilla, H. D., Alfano, O. M., Pérez-Moya,  
515 M., 2015. Photonic efficiency of the photodegradation of paracetamol in water by the photo-  
516 Fenton process. *Environ. Sci. Pollut. Res.* 22, 938-945. doi:10.1007/s11356-014-2990-9.

517 Zazo, J. A., Casas, J. A., Mohedano, A. F., Rodríguez, J. J., 2009. Semicontinuous Fenton oxidation of  
518 phenol in aqueous solution. A kinetic study. *Water Res.* 43, 4063-4069.  
519 doi:10.1016/j.watres.2009.06.035.

---

520 Zhou, W., Zhao, H., Gao, J., Meng, X., Wu, S., Qin, Y., 2016. Influence of a reagents addition strategy  
521 on the Fenton oxidation of rhodamine B: control of the competitive reaction of  $\cdot\text{OH}$ . RSC Adv.  
522 6, 108791-108800. doi: 10.1039/C6RA20242J.

523